Scientific paper

A Mat Based on PVA Doped with TiO_2 Nanoparticles for Removal of Methylene Blue Dye from Aqueous Solution and Improving the Carbon Footprint

Salah M. Abdullah,[1,*] Aseel F. Alwan,[1] Atheer M. Majeed[2] and Suhad A.Yasin[3]

[1] *Polymer Research Unit, College of Science, Mustansiriyah University, Baghdad, Iraq*

[2] *College of Arts, Mustansiriyah University, Baghdad, Iraq*

[3] *Chemistry of Department, College of Science, University of Duhok, Kurdistan Region, Iraq*

* *Corresponding author: E-mail: salah_md@uomustansiriyah.edu.iq*

Received: 08-24-2023

Abstract

Water supply is the great challenge for climate change and overpopulation. A nanofiber mat consisting of polyvinyl alcohol (PVA), nanoTiO_2, and citric acid (PTC) was prepared using an electrospinning technique at a constant flow rate (0.5 ml/h). The morphology of the mat was detected using (FESEM) technique and image J software. The results show that the mat has a nanofiber morphology with an average diameter of 170 nm. This mat was used to remove methylene blue (MB) from water in two ways, the adsorption process and by photodegradation using UV light. The kinetic study of the adsorption of methylene blue MB on a PTC mat was carried out. Results show that the pseudo-second order is the best to describe the adsorption, of MB, and the intraparticle diffusion is the rate determining step. Seven isotherm models; four of two-parameters and three of three-parameters were used to examine the adsorption experimental data by applying linear and non-linear regression methods using six error functions. The results showed comparable data between linear and non-linear regression methods for two parameters isotherms, and the best isotherm fitting with the data were Freundlich and Temkin models. On the contrary, three parameters isotherms showed distracted data between linear and non-linear regression methods. In addition, the results appear that the best predictive error function was Chi-square.

Keywords: Electrospinning, Nanofibers, Adsorption, Photodegradation, Methylene blue, Carbon footprint

1. Introduction

Nanotechnology is one of the versatile fields which can be defined as the ability to control and manipulate nanomaterials and apply them in different fields of industry such as, the biomedical, and food industries.[1,2] The international standardization organization (ISO) defines the nanomaterials as a material that any one of the dimensions must be on a nanometric scale, either the surface or internal structure.[3] The huge expansion in nanotechnology in the last decades contribute to the development of nanofibers with wide applications, especially in medical, agricultural, and environmental fields[4,5,6] Many different methods are used to produce nanofibers such as melt-blown technology, centrifugal spinning, and template synthesis but the most used technique is electrospinning[7]which is a designed process for manufacturing fibers with thin diameters and large surface area[8,9]. This process is proper for polymers (natural and synthetic)[5], inorganic materials, and composites.[10] The electrospinning method is based on the use of electrostatic forces to produce very fine continuous fibers with diameters ranging from nano to micrometers under room temperature and atmospheric conditions.[11,12] The process begins when a high voltage is applied to the polymeric solution that exists in the tip of the metallic needle which induces electrical charges in the polymer droplet leading to the form of a conical droplet which is known as the Tylor cone.[13] When the electric forces overcome the surface tension of the solution, one or more jets are generated and travels towards the collector, the solvent evaporates and nanofibers consequently can be collected.[14,15] The nanofibers resulting from the electrospinning process has a large surface area and the overlapping between these nanofibers leads to the form of a pore structure which makes this fiber an ideal material to be used in a huge number of applica-

tions such as in the biomedical field, tissue engineering, and textiles.[16] Poly (vinyl alcohol) is a well-known polymer with remarkable properties; it is a highly hydrophilic polymer[17] with a high content of hydroxyl groups obtained from hydrolysis of poly (vinyl acetate).[18] It has good chemical, thermal stability[19]and good water solubility,[20,21] PVA is also known as a biocompatible and biodegradable[22,23] polymer, these enthusiastic properties made the PVA one of the most favorable and widely used in the biodegradable materials industry like tissue engineering, drug delivery, and wrapping membrane used in the medical field. Dyes or pigments represent a major challenging problem in the environmental field, especially in developing countries because of their hazardous and toxic effect on living creatures.[24] In the industrial sector, these materials are indispensable due to their wide use in many vital industrial processing like textile, plastic, paper, and cosmetics.[25] The increasing amounts of dyes waste have a bad impact on the ecosystem since dyes are mostly stable compounds against heat and light which means that they degraded slowly in the environment[26,27] and that double the risk of their existence in the waste water. The traditional treatment systems include some techniques like ozonation, filtration, membrane separation, and precipitation.[28,29,30]

The aim is to study the global warming performance or carbon footprint of water production for the residential sector for chemicals as polyvinyl alcohol used in water treatment.

However, some of these methods were highly cost and hard to use on an industrial scale, for example, electrochemical oxidation and coagulation.[31] While the use of the adsorption method in water treatment has superior advantages are beginning from its simplicity, effectiveness low costs, and the possibility of the adsorbent being regenerated.[32] Methylene blue (MB) $C_{16}H_{18}N_3SCl\text{-}3H_2O$ is a cationic dye and the most commonly used dye in the textile industry, when this dye is found in waste water or sewage system it can cause health problems to animals and humans sometimes by inhalation, ingestion, or can cause eye burns by direct contact.[33,34]

In this study, the electrospinning technique used to prepare the PVA mat adopted with TiO_2 nanoparticles and citric acid to enhance the ability of PVA to remove MB dye in two ways by the adsorption process and by photolytic of MB using UV light.

2. Experimental Section

2. 1. Materials

Both of PVA with code no. 63018, and Methylene blue supplied by (Rediel De Haen AG, Seelze, Germany), Titanium dioxide nanoparticles (TiO_2 (with particle size (30 ∓ 5) nm supplied by Changsha S and tech, Citric acid (CA) Chem- supply. Both NaOH granules and HCl with 37% concentration were supplied by (Fluka).

2. 2. Equipment

A double nozzle syringe pump voltage 110-230AC, power frequency 50–60 Hz, (fig. s1), field emission scanning electron microscope (FESEM) supplied by (Hitachi S-570), power sonic410 supplied by Daihan lab tech Co. Ltd (Korea),

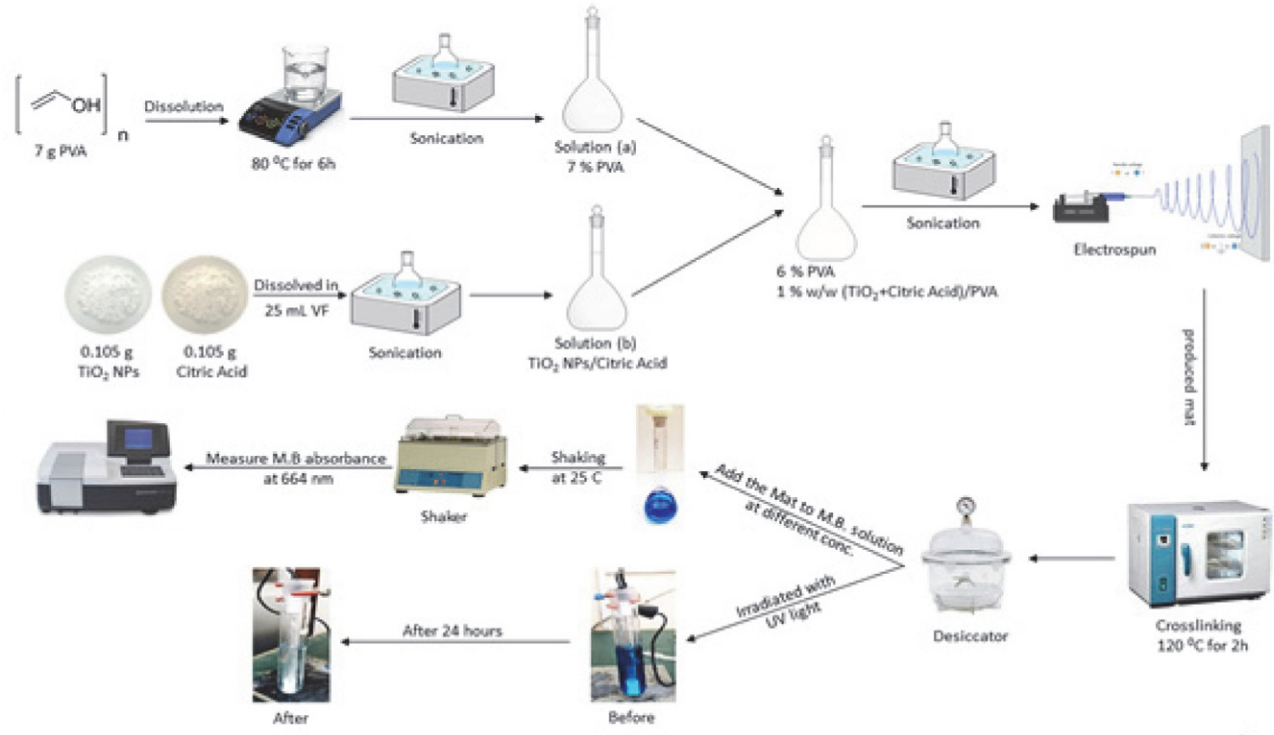

Scheme 1: Synthesis of electrospun PTC mat

UV /visible spectrometer lambda 25 Perkin Elmer. A commercial type UV lamp (made in China) is usually used in reverse osmosis (RO) sterilized water purchased from the Al-Sinak region in Baghdad City, FTIR spectra were recorded on 4200 (JASCO) with a frequency range of (400–4000) cm^{-1}. The pH was measured using a DZS-706A multi-meter (INESA Scientific Instrument Co., Ltd. Shanghai, China).

2.3 Preparation of PTC solution

7 g of PVA was dissolved in 100 ml of hot distilled water at 80 °C to prepare a 7% PVA solution. Equal amounts (0.105g) of both nano TiO_2 and citric acid (CA) were dissolved in 25 ml of distilled water. (6:1) v/v of PVA to CA+TiO_2 solutions were mixed using a sonicator to prepare the (PTC) solution. This solution; consists of 6% w/v of PVA and 1% w/w (TiO_2 and CA) to PVA was used to prepare a PTC mat by electrospinning device.

2. 4. Preparation of PTC Mat Nanofiber

PTC solution was placed into a 5 ml plastic syringe (0.5mm internal diameter needle). The flow rate was 0.5 ml h^{-1}. The distance between the collector and the pump was 10 cm, the electrospinning device was set at 100rpm for the cylinder collector which was wrapped by aluminum foil (see fig. S2), and the applied voltage was adjusted to 25 kV using DC high voltage power source. After that, the produced mat was cured at 120 °C for 2 hours in an oven for crosslinking (See scheme 1 and fig. S3). The morphology of the (PTC) mat was examined by FESEM.

2. 5. Batch Adsorption Study

The adsorption capacity of MB on the electrospun PTC mat was accomplished in a batch adsorption experiment by studying the effect of two different experimental variables, the pH, and the initial MB concentration with a stable weight (0.03 g) of the PTC mat.

2. 5. 1. Study of pH Effect

The initial pH of the MB solutions was adjusted with 0.1 M hydrochloric acid (HCl) and sodium hydroxide (NaOH) to (3, 4.0, 5.8, 6.7, 9.0, 9.8) using a pH meter. A 0.03 g of the PTC electrospun mat was added to each of 10 ml volumetric flasks containing 5 mL of MB solution at certain concentrations. All the solutions were agitating overnight at 25 °C, and 60 rpm. After the adsorption process, the solutions were analyzed by UV spectrometer at 664 nm to estimate the adsorption process.

2. 5. 2. Effect of MB initial concentration

The MB initial concentration (5, 8, 11, 13, 16, 21, 26, and 32 mg l^{-1}) was used to study their effect on the adsorption process with fixed other parameters: the temperature at 25 °C, weight of PTC mat 0.03 g, and the MB solution volume is 10 ml. The amount of dye adsorbed on adsorbent (q_e) and the removal percentage of dye were calculated, respectively, as follows[35]:

$$q_e = \frac{C_i - C_e}{W} V \quad (1)$$

Where *qe* is the amount of dye adsorbed on adsorbent at equilibrium (mg g^{-1}), C_i and *Ce* (mg ml^{-1}) are the liquid-phase concentrations of dye at the initial and equilibrium, respectively. V (L) is the volume of the solution, and W (g) is the mass of the dry adsorbent used.

$$\%\, Adsorption(\%R) = \frac{C_i - C_e}{C_i} \times 100 \quad (2)$$

2. 6. Kinetic Study

The kinetic studies were achieved at the pH of distilled water without any adjustment by immersing 0.03 g of the mat in 10 ml of 15 mg l^{-1} MB solution in a volumetric flask at room temperature with shaking in the shaker and the samples were collected at different time intervals. The decanted solutions were analyzed using a UV-visible spectrophotometer at 664 nm. The aqueous samples were taken at preset time intervals, and the concentrations of dye were similarly measured.

To find the adsorption mechanism, the kinetic models; Elovich model, intra-particle

diffusion, pseudo-first order and pseudo-second-order; were used under optimum conditions : the temperature degree is 25 °C, 10 ml of 15 mg l^{-1} MB solution, pH = 6.5–7, and 0.03 g of absorbent.

$$q_t = \frac{1}{\beta}\ln(\alpha\beta) + \frac{1}{\beta}\ln(t) \quad (3)$$

linear Elovich model[35]

$$q_t = K_{dif} t^{\frac{1}{2}} + B_L \quad (4)$$

intra- particle diffusion[35]

$$\log(q_e - q_t) = \log q_e - \left(\frac{k_1}{2.303}\right) t \quad (5)$$

linear pseudo-first-order[35]

$$\frac{t}{q_t} = \frac{1}{k_2\, q_e^2} + \frac{1}{q_e}(t) \quad (6)$$

linear pseudo-second-order[35]

Where K_{dif} (mg g^{-1} $min^{-1/2}$), K_1 (min^{-1}), and K_2 (g mg^{-1} min^{-1}) are the rates constant for the intra particle diffusion, first-order and second-order respectively, α regarded as the initial adsorption rate (mg g^{-1} min^{-1}), β is the desorption constant (g mg^{-1}), B_L corresponding to the thickness of the boundary layer[35].

2. 7. Error Functions

The set of error functions is used to find non-linear equation parameters of adsorption isotherms models. These function errors are:

Chi- square test (χ^2)[36,37]

$$\chi 2 = \sum_{i=1}^{p} \left[\frac{(q_{e,meas} - q_{e,calc})^2}{q_{e,meas}} \right]_i \quad (7)$$

Sum of squares of the errors (SSE)[38]

$$SSE = \sum_{i=1}^{p} (q_{e,meas} - q_{e,calc})_i^2 \quad (8)$$

A Derivative of Marquard's Percent Standard Deviation(MPSD)[39] :

$$MPSD = \sum_{i=1}^{p} \left(\frac{q_{e,meas} - q_{e,calc}}{q_{e,meas}} \right)_i^2 \quad (9)$$

The Average Relative Error (ARE)[40]:

$$ARE = \sum_{i=1}^{p} \left| \frac{q_{e,meas} - q_{e,calc}}{q_{e,meas}} \right|_i \quad (10)$$

Sum of Absolute Error (EABS)[41]:

$$EABS = \sum_{i=1}^{p} |q_{e,meas} - q_{e,calc}|_i \quad (11)$$

Coefficient of determination (R^2)[39]:

$$R^2 = \frac{\sum (q_{e,meas} - \bar{q}_{e,calc})^2}{\sum (q_{e,meas} - \bar{q}_{e,calc})^2 + \sum (q_{e,meas} - q_{e,calc})^2} \quad (12)$$

Where ($q_{e,meas}$), ($q_{e,calc}$), and ($\bar{q}_{e,calc}$) are the amount in (mg) of MB absorbed at one gram of absorbent experimentally, theoretically, and as average respectively. Try and error method was applied to find the parameters values for three isotherms parameters and also for the non-linear of two parameters isotherm's equations using the Microsoft Excel solver Add-Ins. To solve the non-linear equations, one of the error functions was chosen (except R^2) and fined the parameters of the selected isotherm which gives the minimum value of the choosing error function. Then the other corresponding error functions were calculated depending on the chosen error function. So we get a set of error functions' values. The above process was repeated for other error functions, so each time we get a set of error functions and parameters values for the selected isotherm. To avoid the bias for which the values of parameters are dependent, we divided all the values of error functions to its corresponding maximum value, and this set of resulting values for the error functions was summited. So we get a set of summited values and the one that gives the minimum value was dependent, this method is called the Sum of Normalized Error (SNE).

2. 8. Carbon Footprint

The climate change initiating the drought and the rapid growth of the population with the estimation around 3.5 million people by the middle of the century.[42] It is predicted that by 2030, there will be an imbalance between water supply and public demand if nothing is done to reduce water demand or improve water supply efficiency[41]. To meet future water demand, the demand for electricity and chemicals used to operate these treatment plants will rise. As a result of increased water treatment, GHG (Greenhouse gases) emissions associated with increased energy and chemical consumption will rise.

3. Results and Discussion

3. 1. Characterization

The prepared mat was characterized by FESEM to provide a description of the morphology of the mats and to investigate the nanostructure. The FESEM images in Fig.1 shows that the mat has nanofibers with smooth and fine surface structure. The Image J software reveals that the average diameter of the produced fiber was 170 nm.

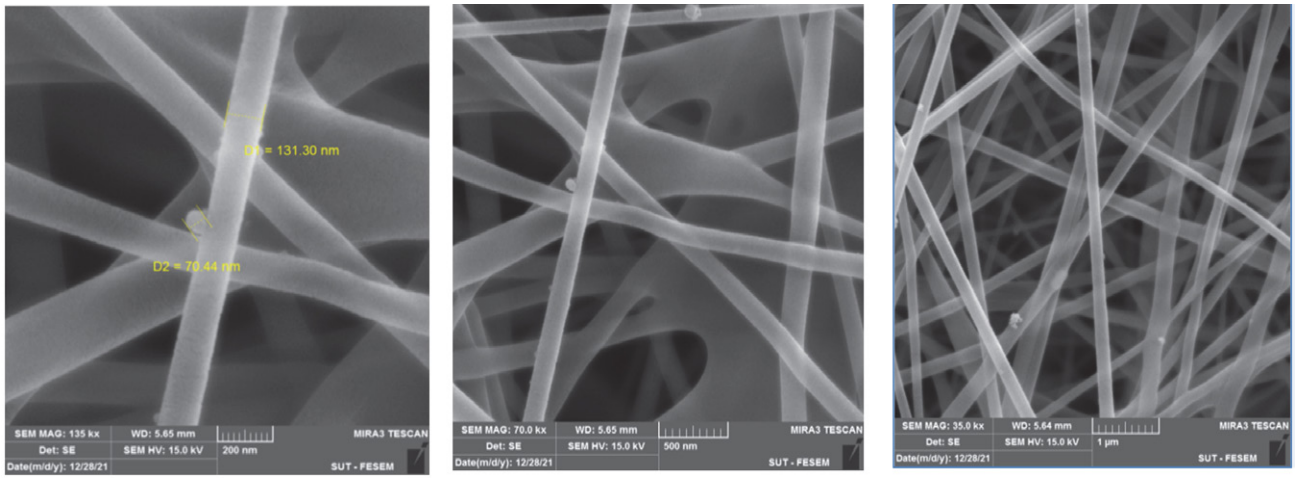

Fig. 1: FESEM images of the prepared (PTC) mat at different resolutions (135 KX), (70 KX) and (35 KX)

FTIR spectra of the PTC mat before and after curing and pure PVA are exhibited in Fig.2 this figure shows the same peaks for all spectra at the studied range (500–4000cm^{-1}) because they have the same functional groups. Whereas the main peaks were observed at 3180–3400 cm^{-1} this peak is related to O–H stretching vibration of the hydroxyl group, peaks 2926 cm^{-1}, 2854 cm$^{-1,}$ assigned to CH_2 asymmetric and symmetric stretching vibration respectively, peak observed at1642 cm^{-1}, peak at 1425 cm^{-1} peak at 1172 cm^{-1}, 1026 cm^{-1} related to C–O stretching of acetyl groups and C-C stretching vibration respectively,[43] A weak peak corresponding to Ti-O stretching appears at 620 cm^{-1} in PTC mat before and after curing.[44]

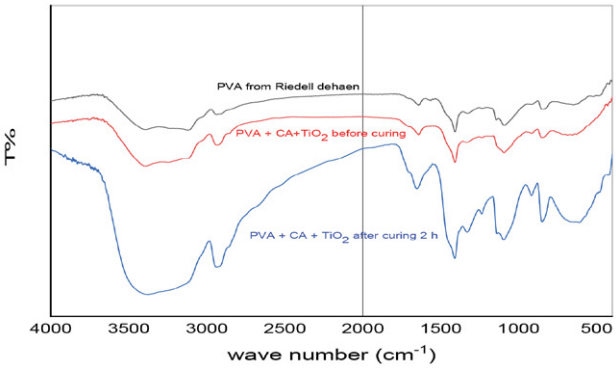

Fig. 2: FTIR spectra of (PTC) nanofibers mat before and after curing and pure PVA

3. 2. Effect of pH

The pH of the dye solution is an essential factor that plays an important role in controlling the whole adsorption process, especially in adsorption capacity.[45] Fig.3 illustrates the effect of pH on the adsorption of MB onto the PTC mat. The effect of the initial pH of the dye solution on the quantity of the dye absorbed was studied by using different pH values under other constant parameters.

When the pH increased from 4 to 6.4, the adsorption capacity increased from 0.3 to 0.77 mg g^{-1}. The adsorption system contains three functional groups, amines from the methylene blue, hydroxyl, and carboxyl group from the PTC mat. In the acidic medium, the amine group in MB will interact with the H^+ in the solution so there is a low chance to interact with the –COOH group in the PTC mat leads to low adsorption of MB, while, In the basic solution, there are free amine groups so it can interact very easy with $–COO^-$ group so the adsorption of MB will increase. When the pH gradually increased towards more basicity the adsorption of MB stays almost constant with a little decrease in the adsorption, this may refer to the bonding of amine groups in MB with OH groups in the solution due to decreasing MB adsorption.

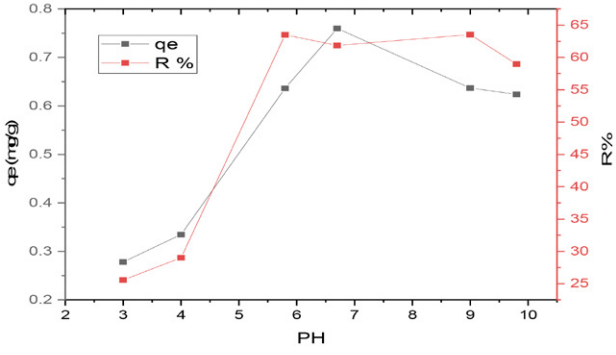

Fig 3: The pH effect of the MB amount adsorbed onto (PTC) mat

3. 3. Effect of Initial MB Concentration

The initial concentration effect of the MB dye adsorbing onto the (PTC) mat was studied between (5 to 32 mg l^{-1}). The adsorption capacity (q_e) of the (PTC) mat increased with the increase the initial MB, while the percent of adsorption (%R) increased with the increasing of the initial MB concentration and reached the maximum point at 15.75 ppm and after that R% gradually decreased with the increasing of MB concentration, as shown in fig. 4.The explanation of this behavior is with increasing of the MB concentration, the adsorption of the dye on the free sites of the mat increased leading to increasing the value of q_e and %R (eqn.1and 2). Until reaching the sites fully saturated. The continuous increasing in MB concentration did not produce any other adsorption of the dye that conduct to decrease in %R value and continuous increasing of q_e values (eqn. 1 and 2).

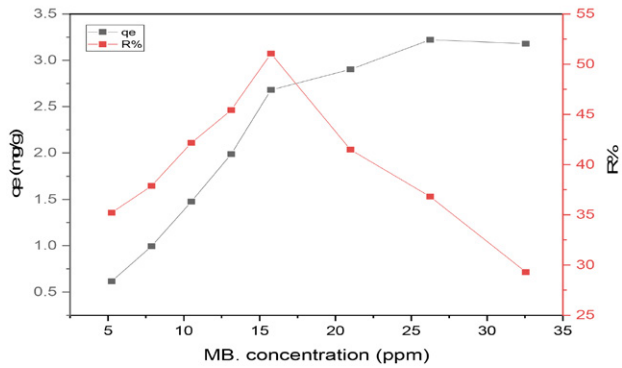

Fig.4: The relationship between MB concentration with (q_e) and R%

3. 4. Effect of Contact Time

Contact time is also one of the important factors that deal with the removal of the dye from the waste water. Fig. 5 shows the relationship between time with adsorption amount (q_e) and the percent of adsorption (%R). In the beginning, the rate of the MB adsorption is very fast due to there being a lot of free sites on the mat until reaches 120 min. after that, the number of free sites will decrease so the

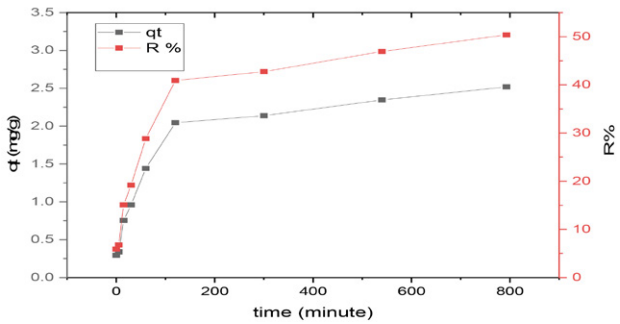

Fig. 5: The time effect for the MB adsorption onto PTC mat

rate decreased until reaching the equilibrium point at 800 min. which represents the best color removal, this behavior is the most common in adsorption studies[46].

3. 5. Find the Location of Adsorption Sites

To find out the sites that MB adsorb onto PTC mat, three types of mats were prepared which are: (A) PVA with TiO_2 mat, (B) PTC mat without curing, and (C) PTC mat with curing at 120 °C for 2 hours. The adsorption process was carried out at optimum conditions (0.03 g of mat, 15 ppm of MB concentration, and pH = 7 at ambient temperature) using these mats, the results showed that the PTC mat with curing gave the highest amount of MB adsorption while the other mats barely gave adsorption that indicates without any doubts, the adsorption of MB was carried out on the site of –COOH groups on the mat which earned from CA. Moreover, to improve the crosslinking was achieved, two pieces of (B) and (C) PTC mats were immersed in distilled water at 80 °C for two hours, and it was found that the (B) mat was completely dissolved while the (C) mat did not.

3. 6. Photolytic study

The photolytic study was carried out using a UV lamp in a quartz tube. A strip of PTC mat collected on an aluminum foil was immersed in a Pyrex tube containing 100 ml of 15 mg l^{-1} of MB dye solution. The color of the MB solution (deep blue) disappeared gradually with irradiation time until reached a colorless solution after 24 hours (see Figs S4, S5, and S6). This result agrees with many studies of TiO_2/UV system for decolourization of (MB) from an aqueous solution.[47]

3. 7. Kinetic Study:

3. 7. 1 Pseudo-first Order and Pseudo- Second Order

Table 2, figures S7 and S8 illustrate the obtained results of pseudo-first order and pseudo- second order for adsorptions of MB on (PCT) mat at optimization condition.

The pseudo-second order has a higher value of correlation coefficient R^2 (0.995) than for pseudo first-order is (0.961), also the value of $q_e$cal. for pseudo-second order is (2.65 mg g^{-1}), these values are very close to the $q_{e\ meas.}$ (2.66 mg g^{-1}) while the value of $q_e$cal. for pseudo-first order (1.99 mg g^{-1}) is too far from the $q_{e.\ meas}$ value so the system obeys without any doubt the pseudo second order.

3. 7. 2. Elovich Equation

The first one who proposed the Elovich equation was Roginsky and Zeldovich[61]. It is used satisfactorily for chemisorption kinetic and heterogeneous surface.[62]

In this, model when we plot (q_t) against, ln(t) we get a straight line with intercept (–0.7213), slope equal to (0.4578), and the R^2 value is 0.9697 (see figure S9). The desorption constant value (β) is 2.1841 g mg^{-1} and the initial adsorption rate (α) is 0.0947 mg g^{-1} min^{-1}. (see table 2), these results showed a good match with the Elovich equation which that indicates to the adsorption is a chemical process and heterogeneous surface of the mat.

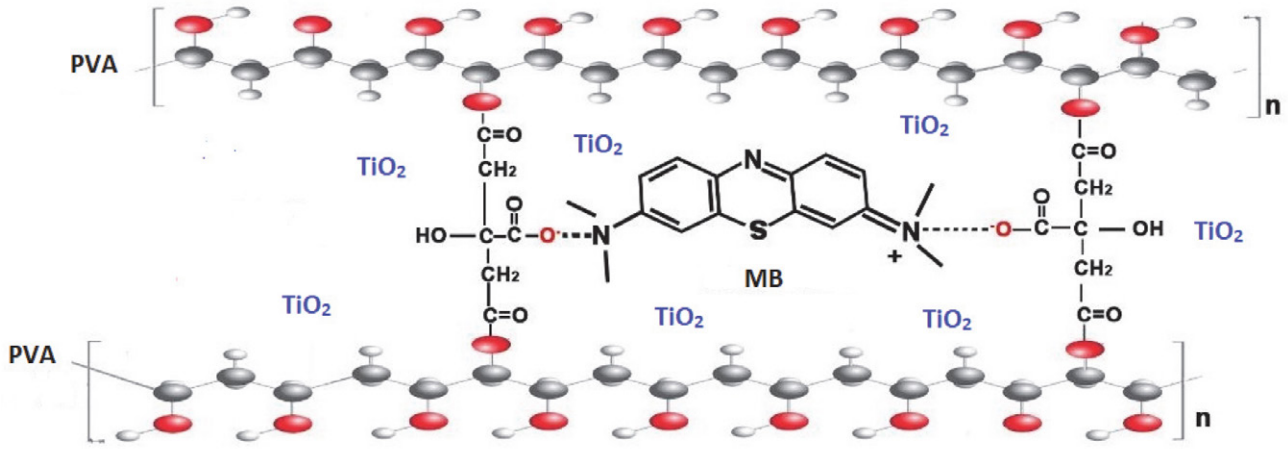

Fig. 6: Illustrate the adsorption site of MB onto PTC mat

Table 1: The previous works for MB batch adsorption

Adsorbent adsorption	Capacity (mg g^{-1})	References
Neem leaf (Azadirachtaindica)	8.76	2005[48]
Bamboo	454.2	2007[34]
Kaolinite	3.05	2009[49]
Bentonite	9.12	2011[50]
Pea shell	246.91	2013[24]
Corn husk	662.25	2013 [51]
Keratin	170	2014[27]
cross-linked chitosan/bentonite composite	142.9	2015[52]
heteroatom-codoped porous carbon	100.2	2018[53]
**VACFF-1300	256.1	2019[54]
VACFF-1600	325.8	2019[54]
Activated carbon from coffee husk	6.82	2020[33]
*DDAB-BC	164	2020[55]
Polylactic acid membrane	97	2020[25]
PLLA/PANI	135	2020[25]
Polyaniline (PAN)	115	2020[25]
PAN/PANI	140	2020[25]
Magnolia denudate leaves(MDL)	185.19	2020[56]
Magnolia grandiflora leaves (MGL)	149.25	2020[56]
Michelia figo leaves *(MFL)*	238.10	2020[56]
PVA/CMC/halloysite nanoclay	8.29	2020[57]
***Nano-Carbon adsorbent	118.98	2022[58]
Molybdenum Disulfide nanomaterials	200	2022[59]
Red mud	147.71	2022[60]
Nano cellulose	4.5	2022[35]
magnetized corn cobs (MCC)	13.23	2023[46]
This work	2.66	

* didodecyldimethylammonium bromide – brown clay. **viscose activated carbon fiber felets. ***zinc gluconate and citric acid

Table 2. Illustrate the kinetic parameter for the linear equation of the kinetic model at optimum conditions and the q_e meas. = 2.6647 mg g^{-1}

Kinetic model	Kinetic parameters		
Pseudo-First order	**$q_e$cal. (mg.g^{-1})**	**K_1 (min^1)**	**R^2**
	1.992	0.0025	0.961
Pseudo-Second order	**$q_e$cal. (mg.g^{-1})**	**K_2 (g.mg^{-1}. min^{-1})**	**R^2**
	2.652481	0.004228	0.995
Elovich model	α (mg.g^{-1} . min^{-1})	β (g. mg^{-1})	R^2
	0.0947	2.1841	0.9697
Intra-particle diffusion	**B_L(mg.g^{-1})**	**K_{dif} (mg g^{-1} $min^{-1/2}$)**	**R^2**
	0.3258	0.0755	0.9268
Part A	**0.0099**	**0.1213**	**0.982**
Part B	**1.4458**	**0.0324**	**0.954**

3. 7. 3. Intra-particle Diffusion (IP) Model

The IP model was used to determine the rate limiting step. Table 2 shows the result of applying this model. Plotting qt against ln(t) gives a straight line with R^2 equal to 0.9268 and the line does not pass through the origin. because the IP model includes a different mechanism that dominance the adsorption process for this reason there are two linear sections (see figure S10) part A: represents the adsorption process from the start to 300 minutes with a very small intercept (B_L = 0.0099) and have high R^2 value

(0.982), that represent the external surface adsorption or instantaneous adsorption stage, while part B: represent the adsorption process from 300 to1035 minutes, which attributed to the gradual adsorption stage, where intra particle diffusion is rate-controlled.[63] At this period the thickness of the boundary layer increase (B_L = 1.4458), so the resistance to the external mass transfer increase as the boundary layer increase.[64] In addition, the rate constant of the intra-particle diffusion K_{dif} will decrease (from 0.1213 to 0.0324) leading to a decrease in the rate of adsorption. At this part, the surface adsorption is more participative in the rate determining step.[65]

3. 8. The Adsorption Isotherm Models

The distribution of the solute molecules between two phases; sold phase (adsorbent) and the liquid phase; at an equilibrium state, can be represented by the isotherm models.

Table S1 shows the entire isotherm models used which include two and three parameters. The obtained results from the applied adsorption isotherm model using Error functions and SNE method for adsorption of MB on (PTC) illustrated in table 4.

a) Two parameter model:

1) Freundlich Isotherm:

Figures S11, S12, and Table 4 show the results of linear and nonlinear Freundlich isotherm equations for the adsorption of MB at ambient temperature. The results show high values of the coefficient of determination R^2 (0.975 and 0.994) for linear and non-linear equations respectively.in addition, the values of Freundlich equations constants (n, K_f) are very close to each other for linear and non-linear expressions. so that the adsorption of MB onto the (PTC) mat obeys the Freundlich isotherm model.

2) Langmuir Isotherm:

The plot of non-linear and linear equations for Langmuir isotherm is shown in figures S13 and S14 respectively. Despite, the Langmuir Isotherm having a higher value of determination coefficient R^2 (0.9998) for linear form (see Table 4) it is not suitable for our adsorption system due to unreasonable values (negative values) of q_{max} and K_L. Also, there are big differences between these values for linear and non-linear forms.

3) Dubinin- Radushkevich isotherm:

Figures (S15-S16) and Table 4 show the results of non-linear and linear Dubinin-Radushkevich isotherm for the adsorption of MB at ambient temperatures. Investigation of these results leads to that the linear regression of Dubinin-Radushkevich isotherm has R^2 values equal to 0.91 for each linear and non-linear. Also, all other parameters are comparable to each other. In addition, the value of adsorption energy (E = 3.75 E + 2 J mol^{-1}) indicates that MB adsorption is a physical adsorption process[66]. But unfortunately, the q_{max} is so small (2.5 mg g^{-1}) and not consistent with practical results.

4) Temkin Isotherm:

For the non-linear form of Temkin isotherm, we plot (q_e) against (C_e), this plot is illustrated in figure (S17) while plot (q_e) against (ln C_e) (figure S18) represents the linear regression of Temkin isotherm. The parameters values for Temkin isotherm (A_t, B_t, b_t) for non-linear; which is obtained according to the SNE method; and linear regression at ambient temperature are shown in Table 4. The values of these parameters are so close and comparable to each other for non-linear and linear regression. Also, the results show an acceptable value of the Coefficient of determination R^2 (0.936, 0.942) for non-linear and linear regression respectively. These results prove that the Temkin isotherm model is a fit with our data.

b) Three parameter model:

The data for the three parameters model; Redlich-Peterson, Sips, and Toth; for linear and non-linear regression at ambient temperature were obtained using trial and error in the solver add-in with Microsoft's spreadsheet, Microsoft Excel. The results show big differences in values for these parameters for linear and non-linear regression for these isotherms that indicate the error does not obey the Gaussian distribution.[67]

1) The Redlich-Peterson Isotherm:

Figure S19 represents the non-linear regression based on the SNE method for the Redlich-Peterson isotherm, while Figure S20 represents the linear form. The values of Redlich-Peterson Isotherm's parameters (K, a, b) for non-linear and linear regression at ambient temperatures are shown in Table 4. In spite of the R^2 value for linear regression being high (0.995) but the exponent parameter value (b) is negative; should be lies between 0 and 1.[68] So the Ridlich Peterson model is not suitable for the adsorption of MB onto (PTC) mat.

2) Sips Isotherm:

The Sips isotherm model is a hybrid model and the most usable three-parameter model for monolayer adsorption[69]. Figures (S21 and S22) represent the non-linear based on the SNE method and the linear regression of Sips isotherm. The results show that the parameters' values (q_{max}, n, b) for the linear and non-linear equations of the Sips Isotherm model at ambient temperature are comparable to each other (see Table 4) and the R^2 values are high (0.995 for non-linear and 0.992 for linear regression). It seems a good fit with our data except the q_m values are so high and not compatible with experimental data.

3) Toth Isotherm:

Figures S24 and S23 illustrate the linear form of the Toth equation which consist of plotting ln $\left(\frac{{q_e}^n}{{q_m}^n - {q_e}^n}\right)$

against (ln C_e) and the non-linear form based on SNE method. (q_{max}, n, K_T) represent the Toth isotherm parameters, and the values of these parameters using a linear and non-linear form of the Toth equation are shown in Table 4. The values of these parameters are so different from each other for linear and non-linear forms and the q_{max} value is very small for the linear form and very high for the non-linear form compared with what we expect from the experimental data, in addition, the Coefficient of determination R^2 values for the linear and non-linear Toth equations are far away from 1 (R^2 = 0.698, 0.865) respectively. So the Toth isotherm is not suitable for application in this adsorption system.

3. 9. Error function

Table 4 shows the value of the sum of the normalized errors SNE for non-linear equations after analyzing five error functions, which are: Sum of squares of the errors (SSE), Chi-square test (χ^2), Derivative of Marquard's Percent Standard Deviation (MPSD), the Average Relative Error (ARE), and Sum of Absolute Error (EABS) using Microsoft Excel solver Add-Ins for minimizing the respective error function across the concentration range studied. Also, the Coefficient of determination R^2 was calculated for linear and non-linear isotherm model equations. The result signed Chi-square test (χ^2) is the best error function according to the SNE method for all non-linear equations (except Dubinin-Radushkevich is MPSD and EABS). This result agrees with Lekan et al.[70] and Neera Singh et al.[71]

3. 10. Carbon Foot Print

The carbon footprint of the optimized composite was calculated using eq 13, where "CO_2-e," "Q," and "F" represent the CO_2 equivalent emission, material amount, and emission factor for producing 1 m^3 of the resultant material, respectively[72,73].

For the improved proposed composites based on citric acid and PVA as the main parameters, the CO_2 equivalent emission is summarized in Table 3. It is clear that all values of CO_2-e is 1.98 kg CO_2-e/m^3. So PTC nanofiber mat is respond to Sustainable Development Goal 17 (SDG 17), especially **6** Clean water and sanitation, **13** climate action.

$$(CO_2 - e) = \sum(Q_1F_1 + Q_2F_2 + Q_nF_n) \quad 13$$

Table 3. CO_2-e Emissions (kg CO_2-e/m^3) for the Proposed PTC

Sample type	Value (kg CO_2-e/m^3) for the PTC	Value (kg CO_2-e/m^3) for the PTC	Total value (kg CO_2-e/m^3)
PVA	2	2 × 0.98 = 1.96	
1.98			
Citric acid	20	20 × 0.01 = 0.2	
TiO_2	0	0.0 × 0.01 = 0.0	

3. 11. Future Prospective

Determination of the optimum conditions for the adsorption of methylene blue. Artificial intelligence (AI)-

Table 4. Parameters of linear and non-linear isotherm models

Isotherm	The parameters for Linear equation				The parameters for nonlinear eqn.					
Two parameters Isotherms										
Frendlich	K_F (mg g^{-1}) (L/mg)$^{1/n}$	N		R^2	K_F (mg g^{-1}) (L/mg)$^{1/n}$	n		R^2	Error function	SNE
	0.0983	0.673		0.975	0.08	0.617		0.994	χ^2	3.683
Langmuir	K_L (L mg^{-1})	q_{max} (mg g^{-1})		R^2	K_L (L mg^{-1})	q_{max} (mg g^{-1})		R^2	Error function	SNE
	–0.0698	–1.97		0.9998	0.0056	42		0.85	χ^2	3.586
Dubinin-Radushkevich	K_{DR} (mol^2 J^{-2})	q_{max} (mg g^{-1})	E (J mol^{-1})	R^2	K_{DR} (mol^2 J^{-2})	q_{max} (mg g^{-1})	E (mol J^{-1})	R^2	Error function	SNE
	3.5E-06	2.5	3.75E+02	0.91	3.55E-06	2.5	3.75E+02	0.91	MPSD,EABS	0.734
Temkin	b_t (J mol^{-1})	A_t (L mg^{-1})	Bt	R^2	b_t (J mol^{-1})	A_t (L mg^{-1})	Bt	R^2	Error function	SNE
	1384	0.3916	1.7897	0.942	1531	0.413	1.618	0.936	χ^2	4.100
Three parameters isotherms										
Redlich-peterson	K(L mg^{-1})	a (L mg^{-1})^b	b	R2	K(L mg^{-1})	a (L mg^{-1})^b	b	R^2	Error function	SNE
	25.78	294.891	–0.575	0.992	0.23	1.00E-05	8.77E-04	0.865	χ^2	3.611
Sips	q_{max}(mg g^{-1})	b(L mg^{-1})	n	R^2	q_{max}(mg g^{-1})	b(L mg^{-1})	n	R^2	Error function	SNE
	200	7.67E-03	0.6256	0.992	316.27	6.15E-03	0.61425	0.995	χ^2	2.221
Toth	q_{max}(mg g^{-1})	K_T (L mg^{-1})	n	R^2	q_{max}(mg g^{-1})	K_T (L mg^{-1})	n	R^2	Error function	SNE
	3	0.117	30	0.698	250	9.18E-04	3.14	0.865	χ^2	3.623

based techniques have been proposed as effective methods for predicting treatment outcomes.

4. Conclusion

A PTC mat with a fiber diameter range of (170nm) was successfully achieved in the electrospinning process, this mat was appropriately used in removing MB dye in two ways; photolytic and adsorption process with optimum conditions (0.03 g of mat, 15 ppm of MB concentration, and pH = 7 at ambient temperature). The Kinetic study of adsorption proves that the adsorption process obeyed the pseudo-second order and good fitting with the Elovich model which indicates the adsorption process is chemical adsorption. Also, the results show the adsorption mechanism follows intra-particle diffusion model. Seven isotherm models having two and three parameters with linear and non-linear regression were investigated and conducted different error functions. The results show that the Freundlich isotherm and Temkin models are the best fit for our data and the Chi-square (χ^2) is the best error function according to the SNE method.

Data Availability:

The figures data used to support the findings of this study are included within the supplementary information file named as the supplementary file; other data are available on request.

Statements and Declaration

On behalf of all authors, the corresponding author states that there is no conflict of interest.

Acknowledgments

The authors would like to thank the Polymer research unit, Mustansiriyah University, Iraq *http://oumustansiriyah.edu.iq* for their support and for providing facilities to accomplish this research work. Also, the authors are thankful for the USAID Partnerships for Enhanced Engagement in Research (PEER) laboratory at the University of Duhok.

5. References

1. Z. H. Mohammad, F. Ahmad, S. A. Ibrahim, S. Zaidi. *Discov. Food.* **2022**, *2,* 12. **DOI:**10.1007/s44187-022-00013-9
2. M. Sirait, Motlan. Innovation in polymer science and technology, IOP Conference, Medan, Indonesia, 2017. *Mater. Sci. Eng.* **2017**, 223. **DOI:**10.1088/1757-899X/223/1/012027
3. D. R. Boverhof, C. M. Bramante, J. H. Butala, S. F. Clancy, M. Lafranconi, J. West S. C. Gordon. *Regul. Toxicol. Pharmacol.* **2015**, *73,*137–150. **DOI:**10.1016/j.yrtph.2015.06.001
4. C. T. Lim, *Prog. Polym. Sci.* **2017**, *70,* 1–17. **DOI:**10.1016/j.progpolymsci.2017.03.002
5. M. Thiruvengadam, G. Rajakumar, I. M. Chung, *3 Biotech.* **2018**, *8,* 1–13. **DOI:**10.1007/s13205-018-1104-7
6. H. Zhong, Z. Li, T. Zhao Y. Chen. *ACS Biomater. Sci. Eng.* **2021**, *7,* 4828–4837. **DOI:**10.1021/acsbiomaterials.1c00982
7. D. H. Kusumawati, K. V. Istiqomah, I. Husnia, N. Fathurin, *J. Phys. : Conf. Ser.* **2021**, 2110. **DOI:**10.1088/1742-6596/2110/1/012010
8. C. Lee, H. Javed, D. Zhang, J. Kim, P. Westerhoff, Q. Li, P. Alvarez. *Environ. Sci. Technol.* **2018**, *52,* 4285–4293. **DOI:**10.1021/acs.est.7b06508
9. J. A. Bhushani, C. Anandharamakrishnan,*Trends Food Sci. Technol.* **2014**, *38,* 21–33. **DOI:**10.1016/j.tifs.2014.03.004
10. R. Sridhara, S. Sundarrajan, J. R. Venugopal, R. Ravichandran**,** S. Ramakrishna, *J. of Biomaterials Sci. Polymer Edition,***2013**, *24,* 365–385. **DOI:**10.1080/09205063.2012.690711
11. S. Parham, A. Z Kharazi, H. R Bakhsheshi-Rad, H. Ghayour, A. F. Ismail, H. Nur, F. Berto, *Materials.* **2020**, *13,* 2153. **DOI:**10.3390/ma13092153
12. M. Kurečič M. S Smole, *Tekstilec,*. **2013**, *56,* 4–12. **DOI:**10.14502/Tekstilec2013.56.4-12
13. J. Rnjak-Kovacina. A. S. Weiss. *tissue Eng.* **2011**, *17,* 365–372. **DOI:**10.1089/ten.teb.2011.0235
14. R. Casasola, N. L Thomas, A. Trybala, S. Georgiadou. *Polymer,* **2014,** *55,* 4728–4737. **DOI:**10.1016/j.polymer.2014.06.032
15. F. Fadil , N. D. N. Affandi , M. I. Misnon, N. N. Bonnia, A. M. Harun M. K. Alam, *Polymers.* **2021**, *13,* 2087. **DOI:**10.3390/polym13132087
16. F. Fadil, F. A Adli, N. D. N Affandi, A. M Harun, M. K. Alam, *Polymers* **2020**, 12, 1–13. **DOI:**10.3390/polym12123043
17. S. Rwei, C. Huang, *Fibers Polym.* **2012**, *13,* 44–50. **DOI:**10.1007/s12221-012-0044-9
18. M. Wang, J. Bai, K. Shao, W. Tang, X. Zhao, D. Lin, S . Huang, C. Chen, Z. Ding , J. YeInt. *J. Polym. Sci.* **2021,** *2021,* 16. **DOI:**10.1155/2021/2225426
19. N. Hasrul, A. Ngadiman, M. Y Noordin, A. Idris, A. S Abdul. I. *Procedia Manuf.* **2015**, *2,* 568–572. ttps://doi.org/10.1016/j.promfg.2015.07.098
20. S. Chen, H. Yang, K. Huang, G. Xiaolong, H. Yao, J. Tang, J. Ren, S. Ren, Y. Ma *Polymers.* **2021**, *13,* 3778. **DOI:**10.3390/polym13213778
21. X. Ji, J. Guo, F. Guan, Y. Liu, Q. Yang, X. Zhang,Y. Xu. *Gels.* **2021**, *7,* 223 **DOI:**10.3390/gels7040223
22. K. Qiu, A. N. Netravali, *Compos. Sci. Technol.* **2012**, *72,* 1588–1594. **DOI:**10.1016/j.compscitech.2012.06.010
23. H. Awada, C. Daneault, *Appl. Sci.* **2015**, *5,* 840–850. **DOI:**10.3390/app5040840
24. Ü, Geçgel, G. Özcan, G. Ç. Gürpınar, *J. of Chemistry*. **2013**, 9.
25. N. Mohammad, Y. Atassi, *Sci. Rep.* **2020**, *10,* 13412. **DOI:**10.1038/s41598-020-69825-y
26. Y. Kuang, X. Zhang, S. Zhou, *Water.* **2020**, *12,* 1–19. **DOI:**10.3390/w12020587
27. A. Aluigi, F. Rombaldoni, C. Tonetti, L. Jannoke, *J. Hazard. Mater.* **2014**, *268,* 156–165.

DOI:10.1016/j.jhazmat.2014.01.012
28. G. Z Kyzas, J. Fu, K. A Matis, *Materials.* **2013**, *6,* 5131–5158. **DOI:**10.3390/ma6115131
29. M. M. Ayad. A. A. El-nasr. *J. Phys. Chem. C.* **2010**, *114,* 14377–14383. **DOI:**10.1021/jp103780w
30. S. A. Yasin, J. A. Abbas, I. A. Saeed, I. H Ahmed. *Polym. Bull.* **2020**, *77,* 3473–3484. **DOI:**10.1007/s00289-019-02919-4
31. A. K. Verma, R. R. Dash, P. A. Bhunia, *J. Environ. Manage.* **2012**, *93,* 154–168. **DOI:**10.1016/j.jenvman.2011.09.012
32. A. Almasia, F. Amirian, M. Mohammadi, A. R. Yari, A. G Dargahi. *Arch Hyg Sci*. **2018**, *7,* 112–118. **DOI:**10.29252/ArchHygSci.7.2.112
33. A. A. Ayalew, T. A. Aragaw, *Adsorption. Sci. Technol.* **2020**, *38,* 205–222. **DOI:**10.1177/0263617420920516
34. B. H. Hameed, A. T. M. Din, A. LAhmed, *J. Hazard. Mater.* **2007**, *141,* 819–825. **DOI:**10.1016/j.jhazmat.2006.07.049
35. A. H. Abdullah, S. Yasin, S. Abdullah, M. Y. Khlaf, I. A. Saeed, *Emergent Mater.* **2022**, *5,* 1199–1212. **DOI:**10.1007/s42247-022-00397-5
36. Y. S. Ho, A. E Ofomaja, *J. Hazard. Mater*. **2006**, *129,* 137–142. **DOI:**10.1016/j.jat.2006.03.012
37. B. Boulinguiez,. P. L. Cloirec, D. Wolbert. *Langmuir*. **2008**, *24,* 6420–6424. ttps://doi.org/10.1021/la800725s
38. K. V Kumar, S. Sivanesan. *J. Hazard. Mater. ,***2006**, *136,* 721–726. **DOI:**10.1016/j.jhazmat.2006.01.003
39. D. W Marquardt, *J. Soc. Ind. Appl. Math. ,*. **1963**, *11,* 431–441. **DOI:**10.1137/0111030
40. B. Subramanyam, A. Das. *J. Environ. Heal. Sci. Eng.* **2014**, *12,* 92. **DOI:**10.1186/2052-336X-12-92
41. Ng, J. C. Y. , W. H. Cheung,G. McKay,*Chemosphere*. **2003**, *6,* 1021–1030. **DOI:**10.1016/S0045-6535(03)00223-6
42. W. K. Biswas, P. Yek, *Renewables Wind. water, Sol.* **2016**, *14,* 1–10.
43. C. Khatuaa, I. Chinyaa, D. Sahab, S. Dasa, R. Sena, A. Dhara, *Int. J. Smart Sens. Intell. Syst.* **2015**, *8,* 1424–1442.
44. E. M Hussein, W. M Desoky, M. F Hanafy, O. W Guirguis, *J. Phys. Chem. Solids*. **2021**, *152,* 109983. **DOI:**10.1016/j.jpcs.2021.109983
45. S. Wang, Y. Boyjoo, A. Choueib, *Chemosphere*. **2005**, *10,* 1401–1407. **DOI:**10.1016/j.chemosphere.2005.01.091
46. N. B Allou, M. A Tigori, A. A Koffi, M. Halidou, N. S. E. P. Atheba, A. Trokourey *Sci. African*. **2023**, *21,* 01828.
47. M. H Abdellah, S. ANosier, A. H El-Shazly, A. A Mubarak, *Alexandria Eng. J.* 2018, *4,* 3727–3735. **DOI:**10.1016/j.aej.2018.07.018
48. G. Krishna. A. S Bhattacharyya, *Dye. Pigment.* **2005**, *65,* 51–59. **DOI:**10.1016/j.dyepig.2004.06.016
49. P. C Mishra, R. K Patel, *J. Hazard. Mater.* **2009**, *168,* 319–325. **DOI:**10.1016/j.jhazmat.2009.02.026
50. C. Perez, D. Fermanndez, A. Bermudez et al. *Chemosphere.* **2011**, *83,* 1028–1034. **DOI:**10.1016/j.chemosphere.2011.01.064
51. M. Khodaie, N. Ghasemi, B. Moradi, M. Rahimi. journal of chemistry. **2013**, 1–6. **DOI:**10.1155/2013/383985
52. Y. Bulut, H. Karaer, *J. Dispersion Sci. Technol.* **2015**, *36,* 61–67. **DOI:**10.1080/01932691.2014.888004
53. B. Chen, Z. Yang, G. Ma, D. Kong, W. Xiong, J. Wang, *Mesoporous Mater*. **2018**, *257,* 1–8. **DOI:**10.1016/j.micromeso.2017.08.026
54. Q. Liu, Y. Zhou, D. Cheng. *Adsorpt. Sci. Technol.* **2019**, *37,* 312–332.
55. M. Munir, M. F. Nazar, M. N. Zafar, et al. *ACS omega*. **2020**, *27,* 16711–16721. **DOI:**10.1021/acsomega.0c01613
56. D. Guo, Y. Li, B. Cui, M. Hu, S. Luo, Y. Liu, *J. Clean. Prod.* **2020**, 267. **DOI:**10.1016/j.jclepro.2020.121903
57. S. Radoor, J. Karayil, J. Parameswaranpillai, S. Siengchin. *J. Environ. Heal. Sci. Eng.* **2020**, *18,* 1311–1327. **DOI:**10.1007/s40201-020-00549-x
58. C. Liang, Q. Shi,J. Feng, et al., *Nanomaterials*. **2022**, 12. **DOI:**10.3390/nano12234235
59. X. Wang, P. Zhang, F. Xu, B. Sun, G. Hong, and L. Bao. *Sustainability*. **2022**, *14,* 7585. **DOI:**10.3390/su14137585
60. Z. Çetinkaya, V. Kalem, *J. Dispers. Sci. Technol.* **2022**, *43,* 1079–1088. **DOI:**10.1080/01932691.2021.1985512
61. S. Z. Roginsky, J. Zeldovich, *J. Acta Physicochim*. **1934**; USSR:554–559.
62. C. W. Cheung, J. F. Porter, G. Mckay, *J. Chem. Technol. Biotechnol.* **2000**, *75,* 963–970. **DOI:**10.1002/1097-4660(200011)75:11<963::AID-JCTB302>3.0.CO;2-Z
63. Y. Li, Q. Du, T. Liu, & A. Wu, *Mater. Res. Bull.* **2012**, *47,* 1898–1904. **DOI:**10.1016/j.materresbull.2012.04.021
64. K. O. Yoro, M. K. Amosa, P. T. Sekoai, J. Mulopo, M. O. Daramola, *Int. J. Sustain. Eng.* **2019**, *13,* 54–67. **DOI:**10.1080/19397038.2019.1592261
65. A. pholosi, E. B. Naidoo, A. E. Ofomaja, *South African J. Chem. Eng.* **2020**, *32,* 39–55. **DOI:**10.1016/j.sajce.2020.01.005
66. J. Monika, V. K. Garg, K. Kadirvelu, *J. Hazard. Mater.* **2009**, *162,* 365–372. **DOI:**10.1016/j.jhazmat.2008.05.048
67. V. Kumar, *Dye. Pigm*. **2007**, *74,* 595–597. **DOI:**10.1016/j.dyepig.2006.03.026
68. N. C. Le, V. P. Dinb, N. C. Le, D. V. Phuc, *Adv. Nat. Sci. Nanosci. Nanotechnol.* **2015**, *6,* 2.
69. R. Saadi, Z. Saadi, R. Fazaeli, N. E. Fard. *Korean J. - Chem. Eng.* **2015**, *32,* 787–799. **DOI:**10.1007/s11814-015-0053-7
70. L. T. Popoola, A. S. Yusuff, O. Adisina, and M. A. Lala. *Journal Environ. Sci. Technol.* **2019**, *12,* 65–80. **DOI:**10.3923/jest.2019.65.80
71. A. Mandal, N. Singh, *J. Environ. Sci. Heal. - Part B Pestic. Food Contam. Agric. Wastes*. **2016**, *51,* 192–203. **DOI:**10.1155/2018/7949741
72. L. F. Jiménez, J. A. Domínguez, R. E. Vega-Azamar, *Adv. Civ. Eng.* **2018**, 2018. **DOI:**10.1021/acsomega.3c00086
73. H. M. Naguib, E. G. Zaki, , D. E. Abdelsattar, A. S. Dhmees, M. A. Azab, S. M. Elsaeed, & U. F. Kandil, *ACS omega,*. **2023**, *8,* 8804–8814.

Povzetek

Oskrba z vodo je velik izziv za podnebne spremembe in prenaseljenost. Podloga iz nanovlaken, sestavljena iz polivinil alkohola (PVA), nanoTiO2 in citronske kisline (PTC), je bila pripravljena s tehniko elektropredenja pri konstantnem pretoku (0,5 ml/h). Morfologijo podlage smo detektirali s tehniko (FESEM) in programsko opremo za slike J. Rezultati kažejo, da ima podlaga morfologijo nanovlaken s povprečnim premerom 170 nm. Ta podlaga je bila uporabljena za odstranjevanje metilen modrega (MB) iz vode na dva načina, s postopkom adsorpcije in s fotodegradacijo z uporabo UV svetlobe. Izvedena je bila kinetična študija adsorpcije metilen modrega MB na PTC podlago. Rezultati kažejo, da je psevdodrugi red najboljši za opis adsorpcije MB, in da je difuzija znotraj delcev korak, ki določa hitrost. Sedem izotermnih modelov; štirje z dvema parametroma in trije s tremi parametri so bili uporabljeni za preučevanje adsorpcijskih eksperimentalnih podatkov z uporabo metod linearne in nelinearne regresije z napako šestih funkcij. Rezultati so pokazali primerljive podatke med linearnimi in nelinearnimi regresijskimi metodami za izoterme dveh parametrov, najboljše ujemanje izoterm s podatki pa sta bila modela Freundlich in Temkin. Nasprotno, izoterme treh parametrov so pokazale moteče podatke med linearnimi in nelinearnimi regresijskimi metodami. Poleg tega rezultati napovedujejo, da je bila najboljša funkcija napovedne napake chi-square test.